Available online at www.sciencedirect.com
SCIENCE DIRECT®
Journal of Nuclear Materials 328 (2004) 55–61
journal of nuclear materials
www.elsevier.com/locate/jnucmat

Sputtering mechanisms near the threshold energy

W. Eckstein, J. Roth *, W. Nagel, R. Dohmen

Max-Planck-Institut für Plasmaphysik, EURATOM Association, D-85748 Garching bei München, Germany

Received 14 November 2003; accepted 6 March 2004

Abstract

Threshold energies for sputtering cannot be calculated directly but have to be evaluated from the energy dependence of the sputtering yields. This paper investigates trajectories of projectile and recoils near the threshold energy for sputtering, where the collision cascade becomes increasingly simple. Statistics of the different collision events show which processes dominate the sputtering close to the threshold energy for selfbombardment of different light and heavy targets. The differential cross-sections for scattering and recoil production explain qualitatively the probability for the various processes.

1. Introduction

Sputtering, the removal of target atoms by collisions induced by bombarding ions or neutrals, has an energy threshold below which the emission of target atoms is impossible. This sputtering threshold depends mainly on the mass ratio, A, of target atom mass-to-projectile atom mass, but also on the surface binding energy, E_s, the angle of incidence, α, and to a lesser extent on the inelastic energy loss of moving atoms inside the solid. For large mass ratios, A, the main process leading to sputtering near the threshold energy is due to reflection of incoming projectiles back to the surface and there removing a target surface atom. The emitted target atoms are in this case primary knock-on atoms, pka, atoms directly removed by backscattered projectiles. This is well documented in [1,2]. For small mass ratios the above mentioned process, (pka, ion out), is less effective, because the reversal of the momentum is more difficult. For normal incidence the momentum has to be changed by more than 90°, so that a target atom is ejected in the process mentioned. Secondary knock-on atoms, ska, are more important at low mass ratios [1,2]. The processes near the sputtering threshold at small mass ratios are discussed in [3,4]. Neglecting electronic energy loss, Yamamura [3] finds the lowest threshold by an infinite series of replacement collisions, whereas it is shown in [4] that the introduction of an inelastic energy loss leads to a limited number of collisions. To get this result some simplifying assumptions in this approach had to be made. The present paper will address the question, which kind of processes is responsible near the sputtering threshold for selfbombardment ($A = 1$). The method of computer simulation is used for this study to determine the trajectories of moving atoms. It is not the aim of this paper to find the most accurate value for the sputtering threshold energy, but to concentrate on the series of collisions, which lead to sputtering near the threshold.

2. Simulation

The simulations are performed using the Monte Carlo program TRIM.SP (version trvmc95) [1,2]. The program was modified to store only those trajectories which lead to sputtered atoms. This is necessary because of our interest in the sputtering process near the threshold, where only a small fraction of collision cascades results in a sputtering event. At the beginning of

* Corresponding author. Tel.: +49-89 3299 1387; fax: +49-89 3299 2279.
E-mail address: jor@ipp.mpg.de (J. Roth).

0022-3115/$ - see front matter © 2004 Published by Elsevier B.V.
doi:10.1016/j.jnucmat.2004.03.010

the calculation, the trajectories of all moving atoms are stored if their energy is larger than the surface binding energy. The trajectories with no sputtered atom are removed after the end of a cascade. This procedure is not straightforward because of the vectorization of the program. Parallel computing has to be used to get reasonable statistics. The parallel program [5] was developed for a CRAY T3E on the basis of the fast proprietary CRAY 'shmem' (shared memory) communication library. Due to the memory space limitations on the CRAY T3E (128 MByte per processor) the program was ported to the IBM Regatta system (3 GByte per processor) with the additional effect of a performance gain of about a factor of six.

The Kr–C interaction potential [6] is used for elastic collisions, an equipartition of the local Oen–Robinson [7] and of the nonlocal Lindhard–Scharff [8] models is assumed for the inelastic energy loss. The heat of sublimation is applied for the surface binding energy in the planar surface binding model, where in the case of selfbombardment the surface binding energy is added to energy of the incident ion (projectile). The planar surface binding model results in a refraction, an increase of the polar emission angle (counted with respect to the surface normal) of sputtered atoms. Because of the restriction in this paper to normal incidence, the projectiles do not experience a refraction. Recoils, target atoms set into motion by energetic projectiles or other target atoms, are created at interatomic distances smaller than the maximum impact parameter, $p_{\max} = \pi^{-1/2}N^{-1/3}$ [2], where N is the target density. Only those recoils are kept whose energy is larger than the surface binding energy. The number of projectiles is typically some 10^9 to get reasonable statistics at low sputtering yields.

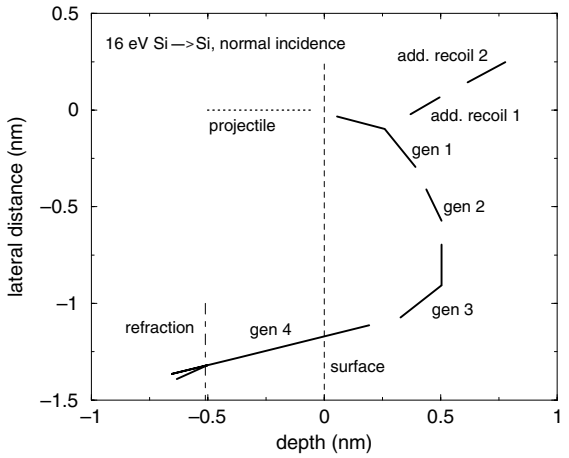

Fig. 1. Trajectory example of 16 eV Si on Si at normal incidence to clarify the nomenclature of additional recoils and generation. The splitting of the trajectory of the sputtered atom outside the target indicates the surface refraction. The target surface is at depth = 0; negative values of depth are outside the target. The trajectories are plotted as projections into the x–y-plane, where x is the depth.

3. Results

The output of the calculation gives the coordinates of the trajectories of both the projectiles and recoils. It further provides the generation of the recoil, the energy of the moving atoms after each collision as well as the elastic and inelastic energy losses, and the direction of the sputtered atom. The calculated results lead to the following characterization of the different sputtering processes. One important distinction is the generation of the atom, which can be sputtered, i.e. the number of newly generated recoils. Generation one is a primary knock-on atom (pka). Sometimes, there is an additional recoil created, which does not lead to sputtering but is stopped in the solid and contributes to the dissipation of the incident energy (see Fig. 1). The trajectories are shown as projections in the x–y-plane (x means target depth). Very close to the threshold the trajectories become planar, otherwise energy would be wasted. Then the trajectories between collisions should be of equal length. This is not exactly the case in Figs. 1 and 2 indicating that the threshold is not yet reached. The distance above the surface, where the refraction is applied, is chosen to be equal to the distance where interactions with target atoms within the solid are taken into account [1,2]. Trajectories for two examples of 25 eV C and 15 eV Au selfbombardment are shown in Fig. 2. Both cases show the trajectories for the most probable process leading to sputtering. The yields are about 2×10^{-7} for both cases (see Table 1). The most striking

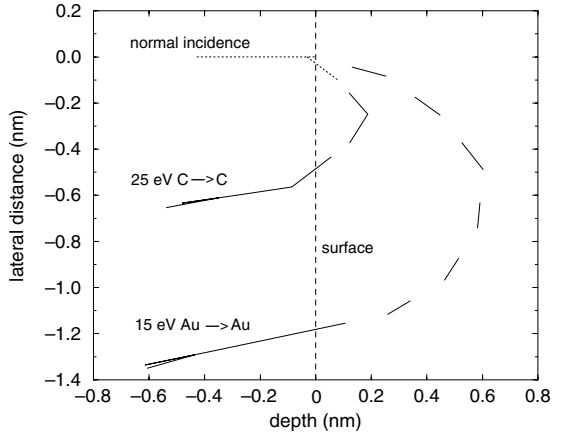

Fig. 2. Trajectories of projectile (dotted line) and recoils (solid lines) for 25 eV C and 15 eV Au selfbombardment at normal incidence. The surface refraction of the sputtered recoil occurs at a depth of −0.35 nm for C and at −0.42 nm for Au.

Table 1
The table provides sputtering yields, Y, and particle reflection coefficients, R_N, for selfbombardment at normal incidence for the species Li, C, Si, Cu, and Au at several incident energies E_0

Element	Density (atoms/nm^3)	p_{max} (nm)	E_s (eV)	E_0 (eV)	Y	R_N
Li	45.98	0.157	1.67	5	1.41×10^{-7}	4.73×10^{-8}
				6	2.87×10^{-6}	1.13×10^{-6}
				8	6.24×10^{-5}	2.02×10^{-5}
C	113.6	0.116	7.41	25	2.18×10^{-7}	3.88×10^{-8}
				26	4.44×10^{-7}	1.13×10^{-7}
				28	1.80×10^{-6}	5.74×10^{-7}
				30	5.27×10^{-6}	1.64×10^{-6}
				32	1.22×10^{-5}	3.47×10^{-6}
				35	3.58×10^{-4}	1.08×10^{-5}
Si	49.78	0.153	4.70	16	3.55×10^{-7}	6.00×10^{-8}
				18	2.44×10^{-6}	4.91×10^{-7}
Cu	84.83	0.128	3.52	14	3.75×10^{-7}	$<10^{-9}$
				18	8.60×10^{-6}	$<10^{-8}$
Au	59.05	0.145	3.80	15	2.33×10^{-7}	$<10^{-9}$
				16	6.18×10^{-7}	$<10^{-9}$
				18	3.11×10^{-6}	$<5\times10^{-9}$
				20	1.24×10^{-5}	$<10^{-8}$
				25	1.45×10^{-4}	4.0×10^{-7}
Au	15.29	0.227	3.80	15	1.31×10^{-7}	$<10^{-9}$

In addition the target density, the maximum impact parameter, p_{max}, and the surface binding energies, E_s, are given.

observation is the difference in the process for C and Au. For Au, a series of replacement collisions (an atom moves to the next collision after it is set into motion, sets another target atom into motion in a collision and stops itself) occurs as was assumed for analytical calculations in [3,4], and in this example a recoil atom of generation 7 is ejected. For the C example, the momentum is reversed in a mixture of scattering and recoil events, and then a recoil of generation two is sputtered. The whole cascade is confined to a shallower depth than in the case of Au. The two examples of C and Au are typical for a light and a heavy element. Examples for other elements are shown in Fig. 6.

Comparing the probability of the different processes in Figs. 3 and 4 shows that in both cases the processes with no additional recoils are dominant close to the threshold energy. The term 'additional recoil' is used for recoils with energies larger than the surface binding energy and which do not contribute further to sputtering; they are stopped in the solid. For C, generation 1 and 2 have the highest probability, for Au it is generation 6 and 7. Even for such low sputtering yields, processes with one additional recoil cannot be neglected. The contributions of the different processes change dramatically with energy as demonstrated for Au selfbombardment. The processes with one and two additional recoils are the strongest contributions for 25 eV Au (see Fig. 4(a)). For 20 eV, it is already the process with no additional recoil and generation 5 and 6 (see Fig. 4(b)), but still with strong contributions of the processes with one and two additional recoils. However, the processes at 15 eV with no additional recoil and generation 6 and 7, are by far the strongest contributions (see Fig. 4(c). Coming closer to the threshold for sputtering, additional recoils become more unlikely (because it would be a waste of energy) and the number of generations is increasing. These considerations make clear that the energy range within a few eV from the threshold has to be covered in order to investigate processes responsible for threshold sputtering. Typical sputtering yields in this energy range are below 10^{-6}.

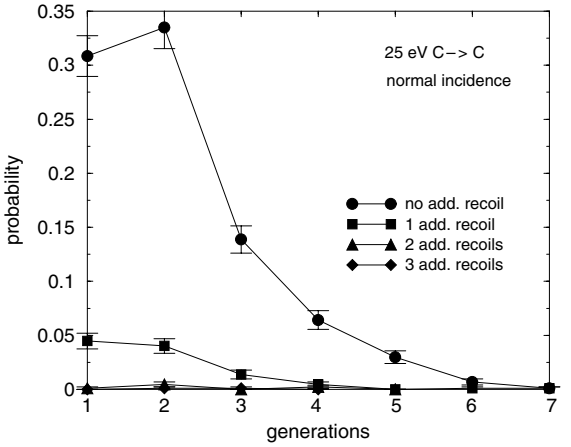

Fig. 3. Probability of different processes versus the generation of sputtered atoms for 25 eV C selfbombardment at normal incidence.

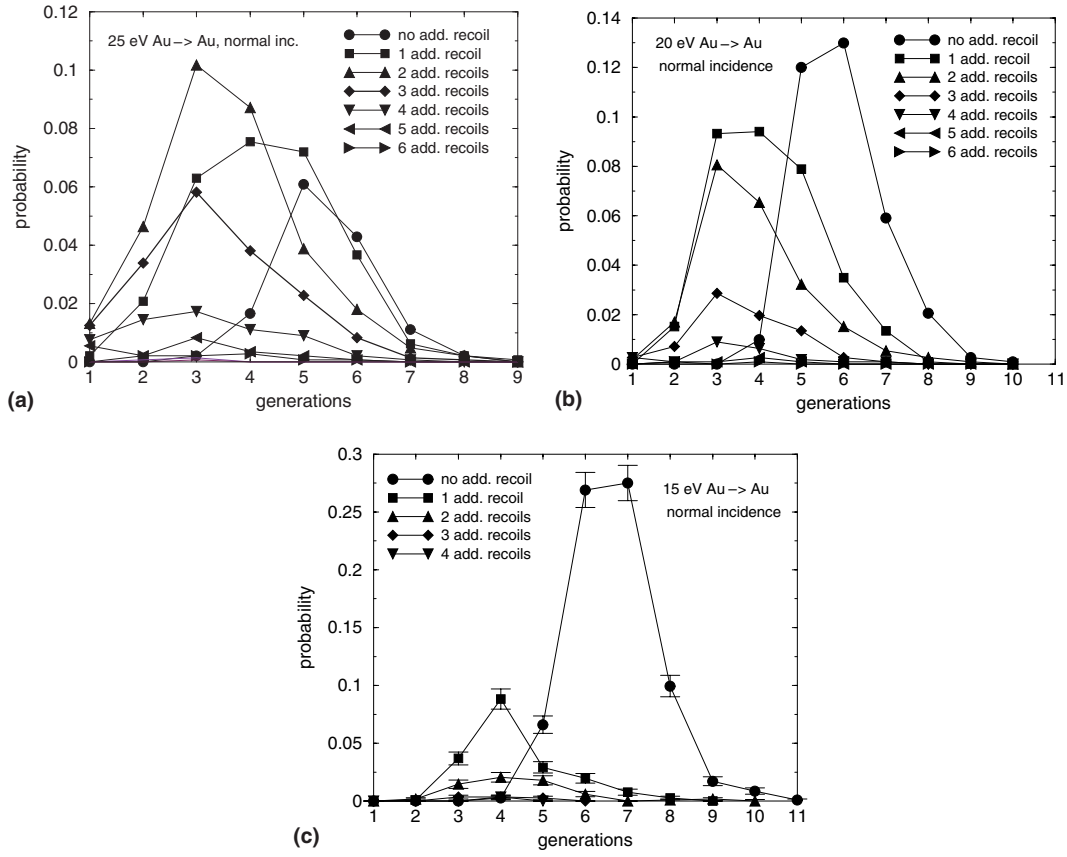

Fig. 4. Probability of different processes versus the generation of sputtered atoms for Au selfbombardment at normal incidence. (a) 25 eV, (b) 20 eV, and (c) 15 eV.

The reason for the difference in the processes for C and Au is the behaviour of the scattering and recoil processes. In order to minimise energy dissipation, the momentum reversal is accomplished in about 8–10 collisions with about 20° deflection, each. In the example of 25 eV C selfbombardment, the average total number of collisions in the solid ($x > 0$) is 4.15, whereas the mean number of projectile scattering collisions is 2.51 and those of recoils is 1.62. For a number of about 4 collisions the scattering or recoil angles are more like 30°. In the case of 15 eV Au selfbombardment the mean number of collisions needed for sputtering is about 8, which gives for the scattering or recoil angle a value of about 13°. The number of collisions for 14 eV Cu on Cu is also found to be about 8, which is in good agreement with the number inferred from Fig. 10b of Ref. [4]. For 15 eV Au on Au, the inelastic energy loss is about 0.6 eV per collision or approximately 7% of the elastic energy loss per collision. The use of an equipartition of the Lindhard–Scharff [8] and the Oen–Robinson [7] inelastic energy losses gives a value of about half of the Lindhard–Scharff losses because of the small values of the Oen–Robinson losses at these low energies. This corresponds to an intermediate value used in [4].

Scattering and recoil angles and cross-sections versus the impact parameter can be determined with a given interaction potential [9,10] which gives the best insight into the processes discussed. Scattering events with these scattering angles require much larger impact parameters than equivalent recoil events. Although the scattering cross-sections are higher than the equivalent recoil cross-sections (Fig. 5(a) and (b)), the required impact parameter in the case of Au is much larger for a scattering event than the maximum possible impact parameter, p_{max}. Therefore, momentum reversal for Au occurs, in a series of recoil processes. For C, the maximum impact parameter allows scattering events of 25°, with a cross-section about four times the equivalent recoil cross-section. Therefore, sputtering events close to the threshold energy for C consist in a mixture of scattering and recoil processes. One should keep in mind, that the impact parameters for a given deflection angle and a corresponding cross-section in Fig. 5(a) and (b) move to larger values with decreasing energy,

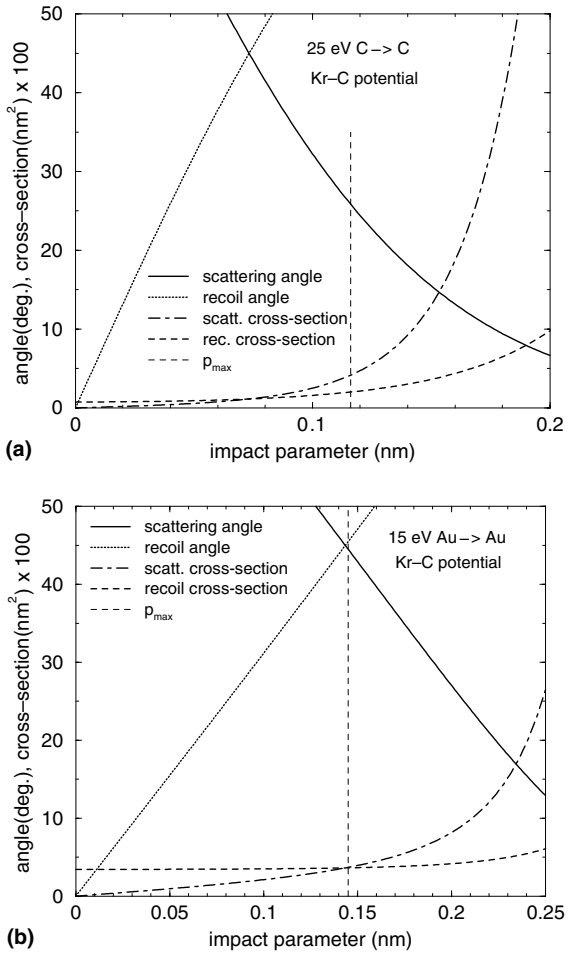

Fig. 5. Scattering and recoil angles, and scattering and recoil cross-sections (KrC potential) versus the impact parameter for (a) 25 eV C selfbombardment, (b) 15 eV Au selfbombardment. The corresponding maximum impact parameters, p_{max}, are indicated.

thus reducing the probability for scattering. The influence of the maximum impact parameter, p_{max}, can be demonstrated by reducing artificially the gold density by a factor of about four to 5 g/cm^3 ($p_{max} = 0.227$ nm) and thus allowing scattering events; this condition produces similar trajectories as for carbon. It is also interesting to note, that the recoil cross-section is nearly constant and mostly larger than the scattering cross-section in the allowed impact parameter range. These considerations explain why replacement collisions occur for Au near the sputtering threshold and why scattering is more important in the case of C. It also makes clear, that a series of scattering events and a final removal of a target atom as speculated in [3] (process 2C) and in [4] are unlikely for selfbombardment at normal incidence.

These considerations are also relevant for the particle reflection coefficient, R_N. Reflection can be considered as the yield for a sputtering event in generation 0, i.e. consisting just in scattering events. R_N is practically zero for the heavy species of Cu and Au but not for the light species of Li, C, and Si, although the particle reflection coefficient is lower than the corresponding sputtering yield for these light species (see Table 1).

Coming closer to the threshold energy, the trajectories are more and more confined to a plane normal to the surface to minimize unnecessary energy loss. Small scattering angles or small recoil angles are optimal, but the adverse effect is the increasing inelastic energy loss, which increases with increasing path length. Therefore, a limited number of collisions leads to the lowest energy consumption for a sputtering process.

A comparison between different species is shown in Fig. 6, where the probability of the process with no additional recoil versus the generation of sputtered atoms at normal incidence for selfbombardment is shown. This process should be the only one possible very close to the threshold energy. Generation 1 and 2 have the highest probability for elements up to Si, whereas for heavier elements generations around 7 are the most common.

As a further consequence of the sputtering processes at these low energies the energy distribution deviates strongly from a Thompson distribution, and the angular distribution is far from a cosine distribution. The energy distribution of sputtered atoms for 15 eV Au on Au shows a maximum at about 0.5 eV, which deviates from the typical value at about half the surface binding energy by a factor of 4 (see Fig. 7). Also, the maximum cutoff energy which is the high energy end of the energy distribution of sputtered atoms, is much lower compared to

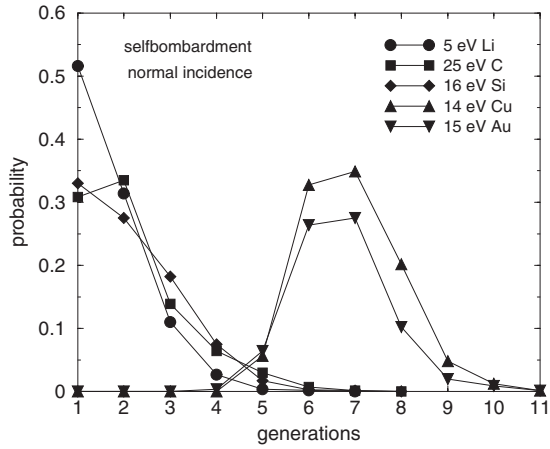

Fig. 6. Process with no additional recoil versus the generation of sputtered atoms for several selfbombardment cases at normal incidence: Li, C, Si, Cu, and Au.

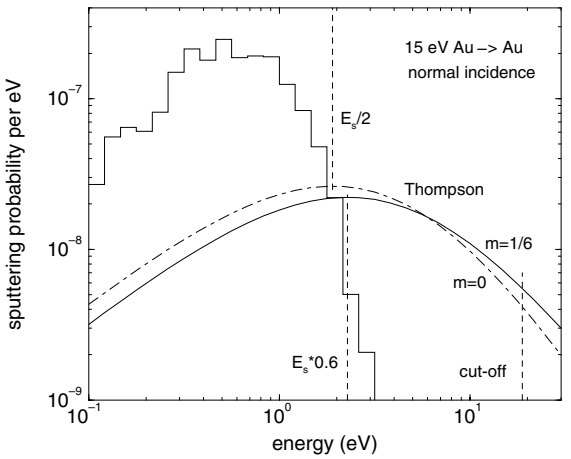

Fig. 7. Energy distribution of sputtered atoms for the bombardment of Au with 15 eV Au at normal incidence. E_s is the surface binding energy. A Thompson distribution is normalized to the total sputtering yield given by the simulation. The Thompson distribution is integrated from zero to the cut-off energy of 18.8 eV ($E_0 + E_s$). The integration is performed for two power potentials with $m = 0$ and $m = 1/6$.

the incident energy than at higher ion energies. Approaching the threshold energy even closer, the maximum cutoff energy and the maximum of the distribution should decrease and finally become zero. The angular distribution of sputtered atoms for the same case exhibit a strong undercosine distribution as demonstrated in Fig. 8. Large exit angles are more probable due to the fact that a momentum change of 180° is more difficult to reach than a momentum change of only 90°.

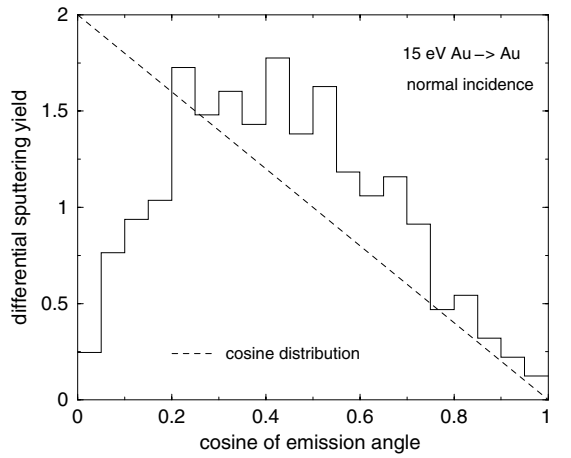

Fig. 8. Angular distribution of sputtered atoms for the bombardment of Au with 15 eV Au at normal incidence. The straight line (dashed) indicates a cosine distribution.

In addition, the refraction by the planar surface potential tends to increase the final exit angle.

4. Conclusions

Sputtering processes for selfsputtering become increasingly simple approaching the threshold energy. The reversal of momentum occurs in a series of collisions leading to deflections of about 20° and avoidance of energy dissipation in additional recoils. The maximum number of collisions is determined by the trade-off of elastic and inelastic energy loss. The processes determining the sputtering threshold become dominant only very close to the threshold, where the sputtering yield decreases to values below 10^{-6}. In order to determine differential distributions at such low yields the TRIM.SP program had to be modified to be run on the new IBM regatta computer. Molecular dynamics would not be able to deliver data for processes with such low probabilities these days.

The present study has shown that the processes leading to sputtering close to the threshold are different for light and heavy element selfbombardment at normal incidence. The important parameter is the maximum allowed impact parameter, which is only dependent on the target density. Scattering events require much larger impact parameters than recoil collisions at the same deflection angle. Scattering is possible for light species, whereas this is impossible for heavy species, where the momentum has to be reversed in a series of replacement collisions.

Differential distributions, such as energy and angular distributions of sputtered atoms deviate strongly from distributions found at higher energies. Although sputtering close to the threshold still requires many collisions of the order of 10 no statistical distribution is established, and emitted atoms have a very narrow energy distribution within 1 eV and an angular distribution favouring emission angles around 70°.

It should be mentioned, that the use of different input parameters, as for example the interaction potential, would lead to different values for the sputtering yield and the particle reflection coefficient in the calculation, especially close to the sputtering threshold energy, where the energy dependence shows such a strong decrease. But the use of other interaction potentials would not change the sputtering processes close to the sputtering threshold energy. Dynamic behaviour could exhibit some changes but this is out of reach because of statistical relevance of calculated data. Crystalline target effects could change the behaviour of collision events, although channeling effects become less pronounced with decreasing energy [11]. Again, this would be difficult to investigate because of the increased computing time of programs which handle crystalline targets.

References

[1] J.P. Biersack, W. Eckstein, Appl. Phys. A 34 (1984) 73.
[2] W. Eckstein, Computer Simulation of Ion–Solid Interactions, Springer Series in Materials Science, vol. 10, Springer, Berlin, Heidelberg, New York, 1991.
[3] Y. Yamamura, J. Bohdansky, Vacuum 35 (1985) 561.
[4] W. Eckstein, C. Garcia-Rosales, J. Roth, J. Làszlò, Nucl. Instrum. and Meth. B 83 (1993) 95.
[5] W. Eckstein, R. Dohmen, Nucl. Instrum. and Meth. B 129 (1997) 327.
[6] W.D. Wilson, L.G. Haggmark, J.P. Biersack, Phys. Rev. B 15 (1977) 2458.
[7] O.S. Oen, M.T. Robinson, Nucl. Instrum. and Meth. 132 (1976) 647.
[8] J. Lindhard, M. Scharff, Phys. Rev. 124 (1961) 128.
[9] M.T. Robinson, Tables of Classical Scattering Integrals, US Atomic Energy Commission, ORNL-4556, 1970.
[10] H.G. Schlager and W. Eckstein, The Scattering Integrals: Integration and Accuracy, IPP Report 9/69, Garching, 1991.
[11] M. Hou, W. Eckstein, Nucl. Instrum. and Meth. B 13 (1986) 324.